

Discrete Step Sizes of Molecular Motors Lead to Bimodal Non-Gaussian Velocity Distributions under Force

Huong T. Vu,¹ Shaon Chakrabarti,¹ Michael Hinczewski,² and D. Thirumalai¹

¹*Biophysics Program, Institute for Physical Science and Technology, University of Maryland, College Park, Maryland 20742, USA*

²*Department of Physics, Case Western Reserve University, Cleveland, Ohio 44106, USA*

(Received 17 August 2015; revised manuscript received 1 April 2016; published 8 August 2016)

Fluctuations in the physical properties of biological machines are inextricably linked to their functions. Distributions of run lengths and velocities of processive molecular motors, like kinesin-1, are accessible through single-molecule techniques, but rigorous theoretical models for these probabilities are lacking. Here, we derive exact analytic results for a kinetic model to predict the resistive force (F)-dependent velocity [$P(v)$] and run length [$P(n)$] distribution functions of generic finitely processive molecular motors. Our theory quantitatively explains the zero force kinesin-1 data for both $P(n)$ and $P(v)$ using the detachment rate as the only parameter. In addition, we predict the F dependence of these quantities. At nonzero F , $P(v)$ is non-Gaussian and is bimodal with peaks at positive and negative values of v , which is due to the discrete step size of kinesin-1. Although the predictions are based on analyses of kinesin-1 data, our results are general and should hold for any processive motor, which walks on a track by taking discrete steps.

DOI: 10.1103/PhysRevLett.117.078101

Molecular motors convert chemical energy, typically from ATP hydrolysis, into mechanical work to facilitate a myriad of activities in the cell, which include gene replication, transcription, translation, and cell division [1–3]. Despite the bewildering variations in their sequences, structures, and functions, a large number of cellular motors take multiple steps directionally along linear tracks and are known as processive motors. Well known in this category are kinesins [4], myosins [5], and dyneins [6] that carry vesicles and organelles along microtubules or actin filaments [7,8] and helicases that unwind nucleic acid strands while translocating on them [9,10]. Fundamental insights into their functions have emerged from single-molecule experiments [2,11–19] combined with discrete stochastic (or chemical kinetics) models [20–24]. These studies have focused on quantities like mean velocity, mean run length, and the dwell-time distribution [18,25], at varying external forces and ATP concentrations. However, much less attention has been paid to distributions of motor velocities in experiments or in theoretical models. Given the inherently stochastic nature of the motor cycle, velocity fluctuations must play an important role in motor dynamics. However, up to now, analytical tools to interpret the fluctuation data, readily available from experiments, do not exist. This Letter addresses that gap, providing universal closed-form expressions for velocity and run length distributions valid for any processive motor.

Let us assume a motor takes steps of size s on a polar track and moves a net displacement ns before detaching at time t , where n is an integer known as the run length. Then the natural definition for the average velocity for

the trajectory is $v = ns/t$. Our work tackles several key questions about the distributions $P(v)$ and $P(n)$ for molecular motors under force. When can $P(v)$ be represented by a Gaussian, an approximation used to analyze experiments [13,14,26–29]? If the detachment rate from the polar track γ is negligible compared to the forward rate k^+ [Fig. 1(b)] the motor walks a large number of steps forward before detachment, then $P(v)$ should approximately be a Gaussian, as expected from the central limit theorem (CLT). However, what is the behavior of $P(v)$ and $P(n)$ when γ becomes comparable to or even larger than the other rates involved, situations encountered in single-molecule experiments in the presence of an external force [Fig. 1(c) [2,30]]? To address these questions, we derive exact analytical expressions for $P(n)$ and $P(v)$, using a simple but accurate kinetic model with only three rate parameters [Fig. 1(b)]. The model has a broad scope, allowing the analysis and prediction of experimental outcomes for a large class of processive motors and other rotary machines.

The central results of this work are the following. (i) At nonzero F , $P(v)$ is non-Gaussian, because γ cannot be neglected compared to k^+ , resulting in the number of steps being not large enough for the CLT to be valid. Even when $F = 0$, there is a discernible deviation from a Gaussian distribution. (ii) Surprisingly, when $F \neq 0$, $P(v)$ is asymmetric about $v = 0$ with a bimodal shape containing peaks, one at $v > 0$ and the other at $v < 0$. With increasing F , the peaks become symmetrically positioned with respect to $v = 0$ and completely symmetric at the stall force F_S . (iii) As F exceeds F_S , reaching the superstall regime, the peak position at $v > 0$ ($v < 0$) moves to higher (lower)

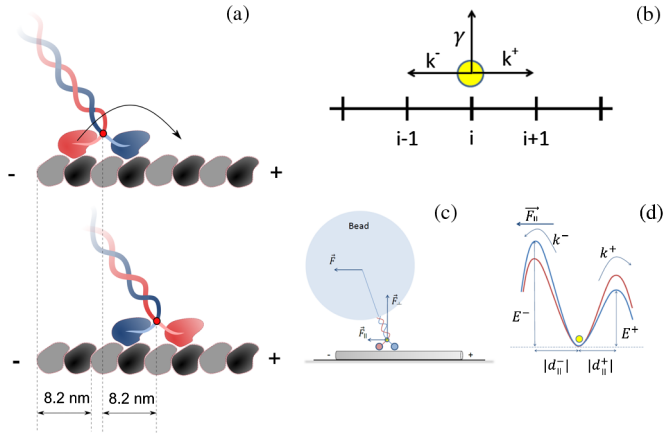


FIG. 1. (a) Schematic of a kinesin molecule walking hand over hand on a microtubule (MT) with a discrete step size of 8.2 nm. (b) Sketch of the model in which the yellow circle represents the center of mass (COM) of the kinesin [capturing the point in red in (a)]. The position of the COM on the MT is denoted by i . Kinesin can step ahead and back and detach from the microtubule with rates k^+ , k^- , and γ , respectively. (c) Decomposition of the resistive optical trap force F applied to the bead attached to the coiled coil, along components parallel (F_{\parallel}) and perpendicular (F_{\perp}) to the MT axis [2]. (d) Energy landscape for forward and backward rates with the blue and the red curves corresponding to zero and nonzero F , respectively. F_{\parallel} increases the backward rate and decreases the forward rate; F_{\perp} increases the detachment rate.

values. These counterintuitive results are consequences of the discrete nature of steps that molecular motors take on their tracks.

In our simplified model [Fig. 1(b)], the motor can move towards the plus or minus ends of the track or detach from each site. The theory with intermediates, required to capture the full complexity of the stepping kinetics observed in experiments, is presented in Supplemental Material [31]. The distribution of times that the motor stays attached to the track is $P(t) = \gamma e^{-\gamma t}$. The probability $P(m, l)$ that the motor takes m forward and l backward steps before detachment is

$$P(m, l) = \left(\frac{k^+}{k_T}\right)^m \left(\frac{k^-}{k_T}\right)^l \left(\frac{\gamma}{k_T}\right) \frac{(m+l)!}{m!l!}, \quad (1)$$

where $k_T = k^+ + k^- + \gamma$ is the total rate, (k^+/k_T) [k^-/k_T] is the probability of taking a forward [backward] step, and (γ/k_T) is the detachment probability. The final term in Eq. (1) accounts for the number of ways of realizing m forward and l backward steps. The run length distribution $P(n)$, where $n = m - l$, is

$$P(n) = \sum_{m,l=0}^{\infty} \left(\frac{k^+}{k_T}\right)^m \left(\frac{k^-}{k_T}\right)^l \left(\frac{\gamma}{k_T}\right) \frac{(m+l)!}{m!l!} \delta_{(m-l),n}. \quad (2)$$

We find that $P(n=0) = [\gamma/(\sqrt{k_T^2 - 4k^+k^-})]$ and $P(n \geq 0)$ takes the simple form (see [31] for details)

$$P(n \geq 0) = \left(\frac{2k^{\pm}}{k_T + \sqrt{k_T^2 - 4k^+k^-}}\right)^{\pm n} \frac{\gamma}{\sqrt{k_T^2 - 4k^+k^-}}. \quad (3)$$

The velocity distribution is given by $P(v) = [\sum_{n=-\infty}^{+\infty}] \times \int_0^{\infty} dt \delta(v - n/t) P(n, t)$, with distances measured in units of step size s . Here $P(n, t) = \sum_{m,l=0}^{\infty} \delta_{(m-l),n} P(m, l, t)$, where the joint distribution $P(m, l, t)$ for m forward and l backward steps with detachment at t is (see [31] for details)

$$P(m, l, t) = \frac{t^{m+l}}{m!l!} (k^+)^m (k^-)^l \gamma \exp(-k_T t). \quad (4)$$

The exact expressions for $P(v \geq 0)$ are

$$P(v \geq 0) = \frac{\gamma}{|v|} \sum_{n=0}^{\infty} \binom{n}{|v|}^{n+1} \frac{1}{n!} (k^{\pm} e^{-(k_T/|v|)})^n \times {}_0F_1\left(; n+1; \frac{n^2 k^+ k^-}{|v|^2}\right). \quad (5)$$

Our approach also allows us to compare $P(v)$ with the distribution of $P(v_{\text{inst}})$ of “instantaneous velocity,” an alternative measure of motor dynamics. If the dwell time of a motor at a site is τ , then $v_{\text{inst}} = s/\tau$. The distribution $P(v_{\text{inst}})$ can, in principle, be computed from $P(\tau)$, the distribution of dwell times [36–38]. Analytical results for $P(v_{\text{inst}})$, discussed in Ref. [31], show that it is not a Gaussian even at $F = 0$, which is the approximate shape expected on general physical considerations.

We first analyze the $F = 0$ data for kinesin-1 (kin-1) [13] using our theory. The motility of kin-1, belonging to a family of motors that walks on microtubule filaments, has been extensively studied since its discovery [39]. Experiments have shown that kin-1 walks hand over hand [40,41], taking discrete steps in multiples of $s = 8.2$ nm with each step being almost identical [11,16,17,42]. The 8.2 nm is commensurate with the α/β tubulin periodicity of a single MT protofilament, here modeled as a one-dimensional lattice [Fig. 1(a)] [4]. For kin-1, the measured $F = 0$ mean velocity is 1089 nm/s [Fig. 2(b)], which implies that

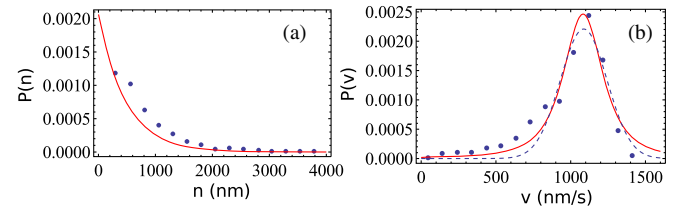


FIG. 2. Simultaneous fits (red lines) of zero force kin-1 data (blue dots) [13] for run length [(a) $P(n)$ —Eq. (3)] and velocity [(b) $P(v)$ —Eq. (5)] distributions. The dashed line in (b) is a Gaussian fit. It should be stressed that the results in (a) and (b) were fit using a single parameter, γ_0 , with the extracted zero force values for k_0^+ and k_0^- in Table I(a).

TABLE I. Force-dependent rates for kin-1. (a) and (b) are rates at $F = 0$ obtained from the experimental data on kin-1 or acetylated microtubule with ratio $(k_0^+/k_0^-) = 221$ [12] and $(k_0^+/k_0^-) = 802$ [43], respectively. The error in γ_0 , obtained by simultaneously fitting $P(n)$ and $P(v)$ (Fig. 1), is estimated using the bootstrap sampling method [44]. (c)–(g) are rates at different values of the load, calculated using the $F = 0$ values in (a).

	F (pN)	k^+ (s^{-1})	k^- (s^{-1})	γ (s^{-1})
(a)	0	133.4	0.6	2.3 ± 0.3
(b)	0	133.0	0.2	2.3 ± 0.3
(c)	3	47.1	1.8	6.2
(d)	4	33.3	2.5	8.7
(e)	5	23.5	3.6	12.1
(f)	7.6	9.5	9.3	29.0
(g)	8.5	7.0	12.8	39.1

$k_0^+ - k_0^- = 132.8$ step/s. The ratio k_0^+/k_0^- is not reported in Ref. [13], which forced us to use data from other sources. Solving these two equations, we get k_0^+ and k_0^- corresponding to two experimental values for $(k_0^+/k_0^-) = 221$ [12] or $(k_0^+/k_0^-) = 802$ [43] [Table I, (a) and (b); note that, even though the ratios are different, k_0^+ and k_0^- are similar]. Using k_0^+ and k_0^- , we obtained the $F = 0$ detachment rate γ_0 by simultaneously fitting the measured [13] velocity distribution using Eq. (5) and run length distribution using Eq. (3). The good fits to both data sets (Fig. 2) using a *single* parameter show that our theory captures the basic aspects of kin-1 motion. More importantly, the value of the only unknown parameter γ_0 is the same in Table I (a) and (b) and in very good agreement with an independent way of obtaining the detachment rate (see [31]). While analyzing the experimental data, we convert the velocity in step/s to nm/s (or vice versa) by multiplying (dividing) by $s = 8.2$ nm.

The distribution $P(v)$ has the same form as in Eq. (5) when the motor is subjected to an external force F [Fig. 1(c)] except $k^+(F)$ and $k^-(F)$ are dependent on F . We model these rates using the Bell model $k^\pm(F) = k_0^\pm e^{-(F_\parallel d_\parallel^\pm)/kT}$, where F_\parallel is the component of the force parallel to the microtubule, k_0^+ and k_0^- are the forward and backward rates at $F = 0$, respectively, and the transition state distances d_\parallel^+ and d_\parallel^- are defined in Fig. 1(d). We can rewrite the arguments of the exponentials as $k^\pm(F) = k_0^\pm e^{-(F d^\pm)/kT}$, defining effective distances $d^\pm = d_\parallel^\pm |F_\parallel|/F$.

We obtained $|d^+| = 1.4$ nm and $|d^-| = 1.6$ nm (Fig. S5), by fitting the average velocity as a function of force [12] with $\bar{v}(F) = [k^+(F) - k^-(F)]$ subject to the constraint $|d^+| + |d^-| = 2.9$ nm [12], assuming that d^\pm are independent of F . Note that $|d^+| + |d^-| = 2.9$ nm is different from the mean step size (8.2 nm) of kin-1, because the force transmitted to the kinesin heads is not parallel to the direction of the motor movement [Fig. 1(c)], so $d^\pm = d_\parallel^\pm |F_\parallel|/F < d_\parallel^\pm$. An alternate mechanism for

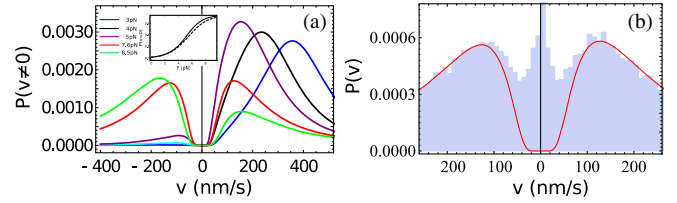


FIG. 3. (a) Predictions of the normalized velocity distributions $([P(v > 0) + P(v < 0)]/[1 - P(v = 0)])$ at different force values. The inset shows $P(v = 0)$ as a function of F . The dashed line is the probability (γ/k_T) that the motor detaches without taking a step. The solid line is the cumulative probability $P(n = 0) = P(v = 0) = [\gamma/(\sqrt{k_T^2 - 4k^+k^-})]$, the total number of motors detaching with zero average velocity and zero net displacement, which includes both motors that detach without stepping and those that return to their starting location. (b) Kinetic Monte Carlo simulations (blue histograms) of the velocity distribution at 7.6 pN load, with a Gaussian step-size distribution, experimentally determined for kin-1 to have a mean of 8.2 nm and a standard deviation of 1.6 nm [17]. The solid lines in both graphs are the exact $P(v)$ —Eq. (5) obtained by assuming that all motors take identical 8.2 nm steps. Although the inclusion of the distribution in the step size leads to minor deviations in $P(v)$, the predicted bimodality persists.

$|d^+| + |d^-|$ being less than 8.2 nm has been proposed elsewhere [45]. Similarly, the F -dependent detachment rate is taken to be $\gamma(F) = \gamma_0 \exp[(F_\perp d_\gamma)/kT]$, which we write as $\gamma(F) = \gamma_0 \exp(|F|/F_d)$, where $F_d = [(|F|kT)/(F_\perp d_\gamma)]$ (≈ 3 pN) is the force at which the two-headed kinesin disengages from the microtubule [30]. At distances greater than the transition state distance d_γ , the motor is unbound from the MT. Table I (c)–(g), listing the three rates at several values of F , shows that $\gamma(F)$ is appreciable relative to $k^+(F)$ at $F > 3$ pN, which has profound consequences on $P(v)$, as we show below.

The normalized $P(v \neq 0)$ distributions for different F values are plotted in Fig. 3(a) using Eq. (5), showing distinctly non-Gaussian behavior, in sharp contrast to the approximately Gaussian distribution at $F = 0$ [Fig. 2(b)]. By stringent standards even at $F = 0$, $P(v)$ is not a Gaussian [46], but the extent of deviation from a Gaussian increases dramatically as F increases. This happens because γ increases and eventually becomes larger than the other rates (Table I), thus decreasing the kinesin's processivity [Fig. S5(d)]. As a result, the CLT does not hold, resulting in $P(v)$ to exhibit non-Gaussian behavior.

More unexpectedly, the predicted F -dependent $P(v)$ are bimodal [Fig. 3(a)]. As F increases, the peak at $v < 0$ becomes higher and reaches the same height as the one at $v > 0$ at the stall force F_S . For forces below $F_S = 7.63$ pN [12], the location of the peak of the $P(v > 0)$ curves, v_p , shifts to lower velocity values as F increases but then moves to higher ones at $F > F_S$ [v_p at $F = 8.5$ pN (green curve) is larger than v_p at $F_S = 7.6$ pN (red curve)].

These two counterintuitive results are direct consequences of the discrete step size of kinesin on the MT. For large values of $\gamma(F)$, corresponding to large forces (where the bimodal structure is most prominent), the time the motor spends on the microtubule is necessarily small [$t \sim 1/\gamma(F)$]. Since ns has to be an integer multiple of 8.2 nm, it cannot be less than 8.2 nm, implying that velocities close to zero (both positive and negative) are improbable, giving us a full explanation of the two-peak structure in $P(v)$. In addition, for $F \leq 5$ pN, v_P can be estimated using $8.2[k^+(F) - k^-(F)]$ nm/s. As F increases, $k^+(F)$ decreases while $k^-(F)$ increases [Table I and Fig. 1(d)], leading to a decrease of v_P with F . However, v_P cannot shift to arbitrarily low values of the velocity due to the discreteness of the step size. As the force increases beyond F_S , for most of the trajectories that contribute to the $v > 0$ peak, the motor falls off after taking just one step (smallest n) [Fig. S5(d)], and at the same time the detachment time continuously decreases, shifting v_P to larger velocities ($v \sim (1/t)$).

The discrete nature of the stepping kinetics is less significant when a large number of n terms contribute to $P(v)$. The results for $P(n)$ in Fig. S5(d) show that, at $F = 0$, kin-1 takes in excess of 50 steps of net displacement before detaching. It is then reasonable to replace the summation in Eq. (5) by an integral. An ansatz for the approximate velocity distribution, $P_A(v)$, which is highly accurate for $F = 0$ where $\gamma \ll k^+$ [Fig. 2(b)], is given by

$$P_A(v > 0) = \frac{\gamma}{v^2} (1 + 4a)^{-1/4} \left[2 \ln \left(\frac{1 + \sqrt{1 + 4a}}{2} \cdot \frac{v}{k^+} \right) - 2\sqrt{1 + 4a} + 2 \frac{k_T}{v} \right]^{-3/2}, \quad (6)$$

where $a = (k^+k^-)/v^2$. However, for $F \neq 0$ the values of γ are such that only a few terms in Eq. (5) are non-negligible, thus making the approximate expression [Eq. (6)] invalid (Fig. S2). As F increases, the average number of forward steps decreases dramatically. At $F = 3$ pN, the probability of kin-1 taking in net displacement for more than ten steps is small. This results in qualitative differences between $P_A(v)$ (continuum steps) and $P(v)$ (discrete steps), which is dramatically illustrated by comparing Figs. 3(a) and S3. Thus, the discreteness of the motor step must be taken explicitly into account when analyzing data, especially at nonzero values of the resistive force.

Although we assumed that stepping occurs in integer multiples of 8.2 nm, experiments show that the step-size distribution has a finite but small width for kin-1 [17], which could possibly affect the bimodal structure in $P(v)$ at $F \neq 0$. Since the inclusion of the distribution in the step sizes makes the model analytically intractable, we performed kinetic Monte Carlo simulations [47]. In this set of simulations, every time the kinesin jumps forward or backward, we assume that the step size has a Gaussian

distribution with mean $s = 8.2$ nm and standard deviation σ , varied from 0 to 8 nm (Fig. S4). As σ increases, the two-peak structure gets washed out. However, for the experimentally measured value of $\sigma = 1.6$ nm, the two-peak velocity distribution is present [Figs. 3(b) and S4(c)] [we converted the standard error $SE = 0.03$ nm from the measurements (see Fig. 2 in Ref. [17]) on wild-type kinesin LpK to $\sigma = SE\sqrt{N} = 0.03\sqrt{2993} = 1.6$ nm]. We conclude that the key predictions in Fig. 3(a) are robust with respect to the inclusion of a physically meaningful step-size distribution, and experiments should be able to discern the two-peak structure in $P(v)$ at $F \neq 0$. The predictions for $P(v)$ at various forces with $\sigma = 1.6$ nm are displayed in Figs. S5(a)–S5(c).

To test the effect of intermediate states, which apparently are needed to analyze the experiments [25], on the bimodality of $P(v)$, we generalized the model to include a chemical intermediate (Fig. S6) and computed $P(v)$ exactly (see [31] for details). We found that the important bimodal feature is still preserved, thus further establishing the robustness of our conclusions.

For $F \neq 0$, the motor would take only a small number of steps, because $\gamma(F)$ is an increasing function of F , raising the possibility that the predictions in Fig. 3(a) may not be measurable. To account for potential experimental limitations, we calculated the conditional probability $P(v|n > n_0)$, which is obtained by neglecting the first n_0 terms in Eq. (5). Figure S10 shows that even with this restriction the bimodal distribution persists, especially near the stall force where it is prominent.

There are substantial variations in force velocity ($F - v$) curves for kin-1 in different experiments. Even the shape of the $F - v$ curve in Ref. [12] does not agree with the results in Refs. [43,48]. For completeness, we analyzed the $F - v$ curves reported in Refs. [43,48]. The theoretical fits are in excellent agreement with the experiments, which allows us to calculate $P(v)$ at $F \neq 0$. The results in Fig. S7 show that, just as those in Fig. 3(a), the predicted bimodality in $P(v)$ remains regardless of the differences in the shapes of the $F - v$ curves among different experiments.

In summary, an exact theoretical analysis using a simple model for motor motility quantitatively explains the zero force velocity and run length distributions *simultaneously* for kin-1, with just one physically reasonable fitting parameter. With an average run length of ~ 632 nm = 77 steps [13], we expect the velocity distribution of kin-1 to deviate from a Gaussian (albeit slightly) even at zero force [46]. Based on the analysis of the zero force data, we calculated the load dependence of the velocity distribution of kin-1 and discovered that the discrete nature of kinesin's steps leads to an unexpected bimodal structure in the velocity distribution under load. This surprising result can be tested in single-molecule experiments, most readily accessed near the stall force where the motor has an equal probability of moving forward or backward. An example

of such a trajectory may be found in Fig. 1 of Ref. [43]. It remains to be seen if our predictions can be readily tested within the precision of single-molecule experiments. Although set in the context of kin-1, our general theory can be used to analyze experimental data for any molecular motor for which the model in Fig. 1(b) is deemed appropriate. As a result, our major results should hold for any finitely processive motor that takes discrete steps.

We are grateful to Steve Block, Changbong Hyeon, and Jonathan Howard for useful discussions. This work was supported in part by a grant from the National Science Foundation (Grant No. CHE 16-36424).

-
- [1] H. F. Lodish, A. Berk, C. A. Kaiser, M. Krieger, M. P. Scott, A. Bretscher, H. Ploegh, and P. Matsudaira, *Molecular Cell Biology*, sixth ed. (Freeman, New York, 2007), p. 973.
- [2] K. Svoboda and S. M. Block, *Cell* **77**, 773 (1994).
- [3] M. Schliwa and G. Woehlke, *Nature (London)* **422**, 759 (2003).
- [4] S. Ray, E. Meyhofer, R. A. Milligan, and J. Howard, *J. Cell Biol.* **121**, 1083 (1993).
- [5] J. A. Spudich and S. Sivaramakrishnan, *Nat. Rev. Mol. Cell Biol.* **11**, 128 (2010).
- [6] A. J. Roberts, T. Kon, P. J. Knight, K. Sutoh, and S. A. Burgess, *Nat. Rev. Mol. Cell Biol.* **14**, 713 (2013).
- [7] J. Howard, *Mechanics of Motor Proteins and the Cytoskeleton* (Sinauer Associates, Sunderland, MA, 2001).
- [8] R. Mallik and S. P. Gross, *Curr. Biol.* **14**, R971 (2004).
- [9] T. M. Lohman, E. J. Tomko, and C. G. Wu, *Nat. Rev. Mol. Cell Biol.* **9**, 391 (2008).
- [10] M. R. Singleton, M. S. Dillingham, and D. B. Wigley, *Annu. Rev. Biochem.* **76**, 23 (2007).
- [11] H. Kojima, E. Muto, H. Higuchi, and T. Yanagida, *Biophys. J.* **73**, 2012 (1997).
- [12] M. Nishiyama, H. Higuchi, and T. Yanagida, *Nat. Cell Biol.* **4**, 790 (2002).
- [13] W. J. Walter, V. Beranek, E. Fischermeier, and S. Diez, *PLoS One* **7**, e42218 (2012).
- [14] S. Courty, C. Luccardini, Y. Bellaïche, G. Cappello, and M. Dahan, *Nano Lett.* **6**, 1491 (2006).
- [15] S. Uemura, K. Kawaguchi, J. Yajima, M. Edamatsu, Y. Y. Toyoshima, and S. Ishiwata, *Proc. Natl. Acad. Sci. U.S.A.* **99**, 5977 (2002).
- [16] K. Svoboda, C. F. Schmidt, B. J. Schnapp, and S. M. Block, *Nature (London)* **365**, 721 (1993).
- [17] A. N. Fehr, C. L. Asbury, and S. M. Block, *Biophys. J.* **94**, L20 (2008).
- [18] M. J. Schnitzer, K. Visscher, and S. M. Block, *Nat. Cell Biol.* **2**, 718 (2000).
- [19] B. Milic, J. O. L. Andreasson, W. O. Hancock, and S. M. Block, *Proc. Natl. Acad. Sci. U.S.A.* **111**, 14136 (2014).
- [20] A. B. Kolomeisky and M. E. Fisher, *Annu. Rev. Phys. Chem.* **58**, 675 (2007).
- [21] M. J. Schnitzer and S. M. Block, *Cold Spring Harbor Symp. Quant. Biol.* **60**, 793 (1995).
- [22] Y. Taniguchi, M. Nishiyama, Y. Ishii, and T. Yanagida, *Nat. Chem. Biol.* **1**, 342 (2005).
- [23] J. W. Shaevitz, S. M. Block, and M. J. Schnitzer, *Biophys. J.* **89**, 2277 (2005).
- [24] D. Chowdhury, *Phys. Rep.* **529**, 1 (2013).
- [25] M. E. Fisher and A. B. Kolomeisky, *Proc. Natl. Acad. Sci. U.S.A.* **98**, 7748 (2001).
- [26] M. Y. Ali, H. Lu, C. S. Bookwalter, D. M. Warshaw, and K. M. Trybus, *Proc. Natl. Acad. Sci. U.S.A.* **105**, 4691 (2008).
- [27] V. Soppina, S. R. Norris, A. S. Dizaji, M. Kortus, S. Veatch, M. Peckham, and K. J. Verhey, *Proc. Natl. Acad. Sci. U.S.A.* **111**, 5562 (2014).
- [28] J. Xu, S. J. King, M. Lapierre-landry, and B. Nemeč, *Biophys. J.* **105**, L23 (2013).
- [29] J. W. Hammond, D. Cai, T. L. Blasius, Z. Li, Y. Jiang, G. T. Jih, E. Meyhofer, and K. J. Verhey, *PLoS Biol.* **7**, e1000072 (2009).
- [30] M. J. I. Müller, F. Berger, S. Klumpp, and R. Lipowsky, in *Organelle-Specific Pharmaceutical Nanotechnology* (Wiley, New York, 2010), pp. 289–309.
- [31] See Supplemental Material at <http://link.aps.org/supplemental/10.1103/PhysRevLett.117.078101> for derivation of the central results, which includes Refs. [32–35].
- [32] M. Abramowitz and I. A. Stegun, *Handbook of Mathematical Functions with Formulas, Graphs, and Mathematical Tables*, ninth Dover printing, tenth GPO printing (Dover, New York, 1964).
- [33] W. O. Hancock and J. Howard, *Proc. Natl. Acad. Sci. U.S.A.* **96**, 13147 (1999).
- [34] A. B. Kolomeisky and M. E. Fisher, *Physica A (Amsterdam)* **279**, 1 (2000).
- [35] H. Wang, C. S. Peskin, and T. C. Elston, *J. Theor. Biol.* **221**, 491 (2003).
- [36] A. Valleriani, S. Liepelt, and R. Lipowsky, *Europhys. Lett.* **82**, 28011 (2008).
- [37] D. Tsygankov, M. Linden, and M. E. Fisher, *Phys. Rev. E* **75**, 021909 (2007).
- [38] M. Linden and M. Wallin, *Biophys. J.* **92**, 3804 (2007).
- [39] R. D. Vale, T. S. Reese, and M. P. Sheetz, *Cell* **42**, 39 (1985).
- [40] A. Yildiz, M. Tomishige, R. D. Vale, and P. R. Selvin, *Science* **303**, 676 (2004).
- [41] C. L. Asbury, A. N. Fehr, and S. M. Block, *Science* **302**, 2130 (2003).
- [42] D. L. Coy, M. Wagenbach, and J. Howard, *J. Biol. Chem.* **274**, 3667 (1999).
- [43] N. J. Carter and R. A. Cross, *Nature (London)* **435**, 308 (2005).
- [44] B. Efron and R. J. Tibshirani, *An Introduction to the Bootstrap* (Chapman and Hall, London, 1993).
- [45] C. Hyeon, S. Klumpp, and J. N. Onuchic, *Phys. Chem. Chem. Phys.* **11**, 4899 (2009).
- [46] J. Hughes, S. Shastry, W. O. Hancock, and J. Fricks, *J. Agric. Biol. Environ. Stat.* **18**, 204 (2013).
- [47] A. Bortz, M. Kalos, and J. Lebowitz, *J. Comput. Phys.* **17**, 10 (1975).
- [48] K. Visscher, M. J. Schnitzer, and S. M. Block, *Nature (London)* **400**, 184 (1999).